PHYSICAL REVIEW A VOLUME 51, NUMBER 6 JUNE 1995

Observation of three-level rectified dipole forces acting on trapped atoms

T. T. Grove, B. C. Duncan, V. Sanchez-Villicana, and P. L. Gould
Department of Physics, Box U-46, University of Connecticut, Storrs, Connecticut 06269-3046
(Received 6 February 1995)

We have observed rectified dipole forces acting on three-level atoms in the cascade configuration. Laser cooled and trapped rubidium atoms are illuminated with an intense bichromatic standing wave (780 and 776 nm) tuned near resonance with the $5S_{1/2}\rightarrow 5P_{3/2}\rightarrow 5D_{5/2}$ transitions. The resulting rectified forces produce periodic potential wells (71-μm period), which localize the cold atoms. Experimental results are in reasonable agreement with theoretical predictions. These forces may be useful in atom optics and laser traps.

PACS number(s): 32.80.Pj, 42.50.Vk, 03.75.Be

The forces exerted by near-resonant laser light have been used to cool, trap, and generally manipulate atoms [1–3]. These techniques have allowed advances in areas ranging from precision measurements to collision physics. A great deal of activity has centered around understanding and improving these forces. In this Rapid Communication, we present measurements of rectified dipole forces acting on a three-level atom in the cascade configuration. These forces can be large and unidirectional over a macroscopic distance, allowing the creation of deep potential wells for neutral atoms.

In general, there are two types of radiative forces on atoms. The spontaneous force (or radiation pressure) is unidirectional but limited in magnitude by the spontaneous emission rate of the atom. The dipole force, on the other hand, is due to the interaction of the induced atomic dipole with the incident electric field. Since it involves stimulated emission, it does not saturate with laser intensity. It is proportional to the gradient of intensity, and therefore tends to be large when the intensity exhibits a rapid spatial variation. However, this means that the force reverses direction on the scale of this variation, preventing the buildup of a deep potential well. For example, in a standing wave, the force changes sign four times in one wavelength.

The idea of a rectified force [4,5] is to prevent the dipole force in a standing wave from changing sign on the optical wavelength scale. This is done by taking advantage of the dispersive nature of the dipole force, i.e., the fact that it changes sign with detuning. If the detuning can be made to change sign when the intensity gradient does, these two sign changes cancel, meaning the force remains unidirectional. In a three-level atom subject to a bichromatic standing wave, as shown in Fig. 1(a), the effective detuning of one transition can be made to change sign via the spatially varying ac Stark shift caused by the other transition. This effect depends on the relative phase $\chi=(k_3-k_1)z$ between the standing waves, so that as the two standing waves get out of phase (which they do on the scale of the beat wavelength) the force will reverse. If the wavelengths of the two transitions are similar, the beat wavelength will be long and the force will be unidirectional over many wavelengths, resulting in a deep potential well for the atom.

Rectified forces exist for all three three-level systems: lambda [6–9], vee [10], and cascade [11]; as well as for a two-level system [4,5]. A unique feature of the cascade configuration [11] is that the rectified force can be large when two-photon resonant, and that in this case, the force can be completely rectified on the wavelength scale, meaning that wavelength-scale channeling is not present. An example is seen in Fig. 2, where we show (a) the wavelength-scale force F, (b) the wavelength-averaged force $\langle F\rangle$, and (c) the potential U. These results are obtained by numerically solving the three-level optical Bloch equations [11] (OBE's). In Fig. 2(a), the wavelength-scale force at $\chi=0.17\pi$ (where $\langle F\rangle$ is maximized) is indeed seen to be fully rectified. This complete rectification persists over a large range centered on the potential minimum ($\chi=\pi/2$) and, as a result, the potential [Fig. 2(c)] has no local minima, which would channel atoms and impede their motion towards $\chi=\pi/2$. If both detunings are reversed (maintaining two-photon resonance), the force changes sign, resulting in a shift of the potential minimum by one-half the beat wavelength.

Previous experiments have demonstrated rectified forces in a two-level system [12,13] and in three-level systems in both lambda [14,15] and vee [16,17] configurations. Deflections of atomic beams were used to measure these forces, which had beat wavelengths of several centimeters.

In the present work, we observe rectified forces acting on laser-cooled and trapped rubidium atoms. To our knowledge, this is the first demonstration of radiative forces in a three-level cascade system. The $5S_{1/2}\rightarrow 5P_{3/2}\rightarrow 5D_{5/2}$ transitions in Rb are interesting because they have nearly identical reso-

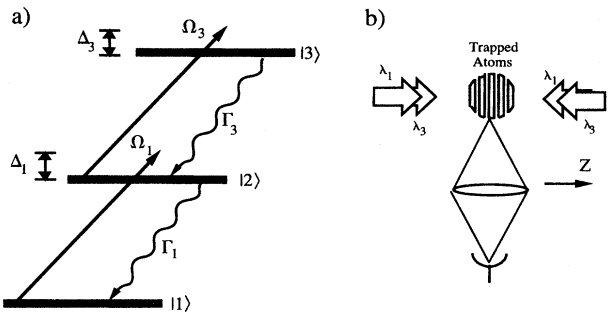

FIG. 1. (a) Three-level cascade system. The detunings are Δ_i (shown as positive) and the Rabi rates are $\Omega_i(z)=\Omega_i\cos k_i z$. For the $5S_{1/2}\rightarrow 5P_{3/2}\rightarrow 5D_{5/2}$ transitions in Rb, the population decay rates are $\Gamma_1=2\pi(5.9\text{ MHz})$ and $\Gamma_3=2\pi(0.66\text{ MHz})$ and the transition wavelengths are $\lambda_1=780.2$ nm and $\lambda_3=776.0$ nm. (b) Schematic of the experiment: a bichromatic standing wave is applied to a sample of trapped atoms and the resulting density modulation is observed.

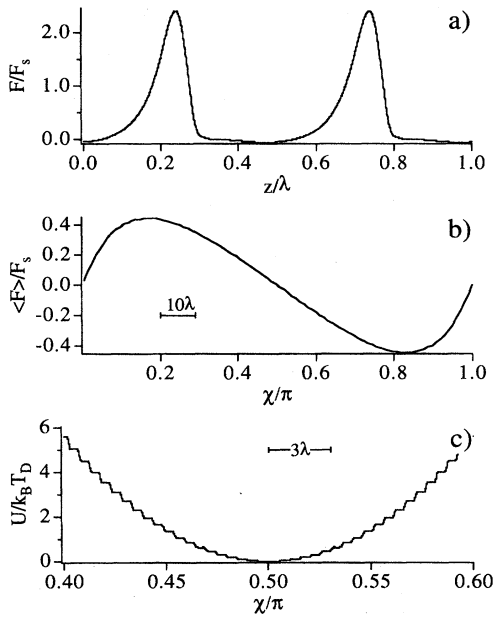

FIG. 2. Example of rectified force acting on the $5S_{1/2} \rightarrow 5P_{3/2} \rightarrow 5D_{5/2}$ transitions in Rb: (a) wavelength-scale force for $\chi = 0.17\pi$, (b) wavelength-averaged force, (c) potential. Parameters are $\Omega_1 = \Omega_3 = 4\Gamma_1$, $\Delta_1 = -\Delta_3 = 2\Gamma_1$. The force is in units of the maximum spontaneous force $F_s = \hbar k\Gamma/2$ and the potential is in units of the Doppler temperature $k_B T_D = \hbar\Gamma/2$. Here $k \equiv (k_1 + k_3)/2$, $\lambda \equiv 2\pi/k$, and $\Gamma \equiv \Gamma_1$. A change in χ of π corresponds to a change in z of 91λ or 71 μm. The average force in (a) is $0.45F_s$ and the well depth in (c) is $87k_B T_D$.

nance wavelengths: 780 and 776 nm. The beat wavelength (i.e., the period of the rectified force) in this case is 71 μm. The basic idea of the experiment is to illuminate the cold atoms with a bichromatic standing wave, as shown in Fig. 1(b), and observe their accumulation in the potential wells formed by the rectified force.

The sample of cold ^{85}Rb atoms is obtained using a magneto-optical trap [18] (MOT) that captures slow atoms from room-temperature vapor [19]. The trap laser is tuned $\sim 1\Gamma$ below the $5S_{1/2}(F=3) \rightarrow 5P_{3/2}(F'=4)$ transition at 780 nm and has an intensity (sum of six beams) of ~ 7.5 mW/cm^2. Optical hyperfine pumping is prevented with a laser tuned near the $5S_{1/2}(F=2) \rightarrow 5P_{1/2}(F'=3)$ transition at 795 nm. These diode lasers (Sharp LTO24MDO) are linewidth narrowed by optical feedback from diffraction gratings at grazing incidence [20], yielding linewidths of ~ 1 MHz. Long-term frequency stabilization is achieved by locking to saturated absorption features. The MOT typically contains $\sim 2 \times 10^6$ atoms at a density of $\sim 10^{10}$ cm^{-3} and loads in ~ 1 s.

The bichromatic field is produced by combining the light from two linewidth-narrowed diode lasers. The laser at 780 nm is stabilized at a variable detuning Δ_1 from the $5S_{1/2}(F=3) \rightarrow 5P_{3/2}(F'=4)$ transition using saturated absorption in a magnetic field [21]. The 776-nm laser is locked at a detuning $\Delta_3 = -\Delta_1$ relative to the $5P_{3/2}(F'=4) \rightarrow 5D_{5/2}(F''=5)$ transition using Doppler-free two-photon two-color spectroscopy with counterpropagating beams in a room-temperature vapor cell [22]. This technique maintains two-photon resonance for arbitrary values of Δ_1. The bichromatic standing wave is created by retroreflecting from a mirror (located ~ 20 cm from the MOT), which can be translated to adjust the relative phase χ between the two standing waves (71 μm changes χ by π). Both fields are circularly polarized in an attempt to drive the stretched-state transitions: $m_F = F \rightarrow m_{F'} = F' \rightarrow m_{F''} = F''$. These Gaussian beams are focused to yield an average size of ~ 700 μm ($1/e^2$ diameter) at the location of the MOT. This is to be compared with the ~ 500-μm size of the trapped atom cloud. The actual focus is beyond the retromirror to compensate for intensity losses from the uncoated vacuum window. The intensities of the counterpropagating pairs are balanced to better than 5% (780 nm) and 20% (776 nm).

In order to clarify the interpretation of the experiments, the MOT laser and the bichromatic field are alternated in time (~ 50-μs period) using acousto-optic modulators (AOM's). The bichromatic field typically has a duty cycle of $\sim 10\%$. This low duty cycle serves three purposes. First, it allows the MOT to continuously capture, cool, and confine the atoms. Second, it results in the temperature being determined primarily by the MOT. Third, the fluorescence from the trapped atoms is dominated by the uniform MOT excitation so that a time-averaged image is an accurate representation of the density distribution. The repumping laser is on continuously to prevent optical hyperfine pumping while the rectified force is being applied. Since it is tuned to the D_1 line, it is immune to ac Stark shifts produced by the relatively intense bichromatic standing wave.

The localization of cold atoms in the rectified-force potential wells results in a density modulation $n(z)$ of the trapped cloud. This fringe pattern is viewed perpendicular to z by a charge-coupled device camera with an $f/6$ lens (unit magnification, resolution ~ 18 μm $1/e^2$ diameter) and a 780-nm bandpass filter (transmission of 50% at 780 nm and 25% at 776 nm). Images with and without the trapped cloud are subtracted in order to reduce scattered light and several (typically 20) images are averaged in order to reduce noise. Profiles of the image along the z axis reveal the density modulation. For a given image, several (typically 10) lines along z are analyzed to yield an average value and standard deviation of the contrast.

Typical fringe patterns are shown in Fig. 3 (inset). For these scans, a smoothed version of the profile is subtracted from the true profile. This difference profile is then divided by the smoothed profile to yield a normalized fringe pattern. The pattern has the expected period (71 μm) and follows the retromirror as it is translated. A crucial test that the modulation is due to the rectified force is to change the sign of both detunings (maintaining two-photon resonance). Theory predicts that the force (and thus the potential) should change sign, resulting in an inversion of the fringe pattern. If the pattern were simply a spatial modulation of the fluorescence (both $5P \rightarrow 5S$ and $5D \rightarrow 5P$) due to changes in the relative phase of the bichromatic excitation, we would expect a modulation at the beat wavelength which would *not* change sign with the detunings [23]. As seen in Fig. 3 (inset), the pattern does indeed reverse with detunings, indicating that the rectified force is responsible for the modulation.

In Fig. 3, we present the results of a more thorough investigation of the detuning dependence of the fringe pattern

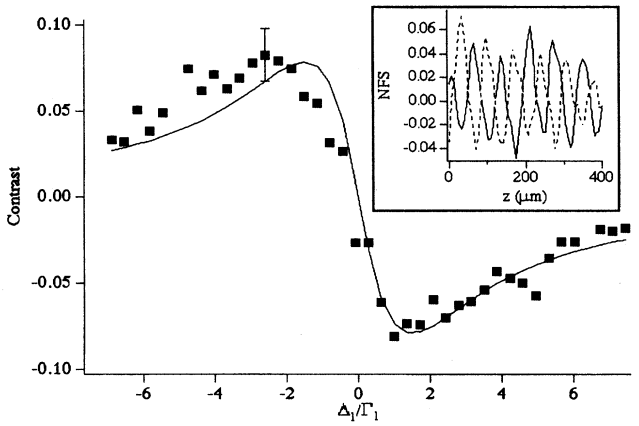

FIG. 3. Contrast as a function of detuning for $\Omega_1=3.1\Gamma_1$ ($I_{peak}=75$ mW/cm^2), $\Omega_3=1.5\Gamma_1$ ($I_{peak}=275$ mW/cm^2). Two-photon resonance ($\Delta_1=-\Delta_3$) is maintained throughout. The solid curve is the fit described in the text. Error bars result from a quadrature combination of the standard deviation from different lines of the image and the uncertainty in assigning contrast to a given line. Inset: normalized fringe signal (NFS) demonstrating fringe reversal with detunings. $\Delta_1=-\Delta_3=2.5\Gamma_1$ (solid curve); $\Delta_1=-\Delta_3=-2.5\Gamma_1$ (dashed curve).

contrast. In order to clearly demonstrate the inversion of the pattern with detunings (as shown in the inset), we allow the contrast to be negative by defining it as the normalized difference between densities at two fixed phases:

$$C=\frac{n(\chi=0)-n(\chi=\pi/2)}{n(\chi=0)+n(\chi=\pi/2)}. \quad (1)$$

For $\Delta_1<0$ ($\Delta_1>0$), the potential minimum is located at $\chi=0$ ($\chi=\pi/2$), resulting in a positive (negative) contrast. We also show in Fig. 3 a theoretical fit to the data. If the cold atoms are in thermal equilibrium, their density distribution in the potential $U(z)$ is described by a Boltzmann factor:

$$n(z)=n_0 e^{-[U(z)/(k_B T)]}. \quad (2)$$

The solid curve in Fig. 3 is based on the potential-well depths obtained from numerical solutions of the OBE's. These well depths are time averaged by multiplying by the duty cycle. The Rabi rates used in the calculations are based on m-averaged and m'-averaged strengths for the $5S_{1/2}(F=3)\rightarrow 5P_{3/2}(F'=4)$ and $5P_{3/2}(F'=4)\rightarrow 5D_{5/2}(F''=5)$ transitions, respectively [24]. The temperature, assumed constant for all the data, is a parameter in the fit. The best least-squares fit yields $T=1.1\pm 0.2$ mK, which is somewhat higher than recently measured (~ 70 μK) for similar trap parameters [25]. However, these previous measurements were made under conditions of low atomic density and with great care taken to balance the MOT beam intensities and ensure that the trap formed at zero magnetic field. Similar precautions were not taken in the present experiment, so this higher temperature is not unreasonable. We note that for the highest contrast shown in Fig. 3 (i.e., for $\Delta_1=\pm 1.5\Gamma_1$) the calculated well depth (for 100% duty cycle) is ~ 1.5 mK.

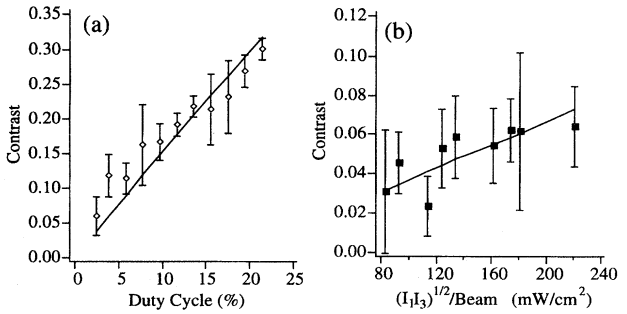

FIG. 4. (a) Contrast as a function of duty cycle for $\Omega_1=4.4\Gamma_1$, $\Omega_3=1.4\Gamma_1$, $\Delta_1=-\Delta_3=-3.7\Gamma_1$. (b) Contrast as a function of laser intensities for $\Delta_1=-\Delta_3=-3.3\Gamma_1$ and duty cycle $=10\%$. The intensity ratio is kept approximately constant at $I_3/I_1\sim 2.7$, resulting in $\Omega_3/\Omega_1\sim 0.4$.

We have also investigated the dependence of the contrast on the duty cycle and the laser intensities. Results are shown in Figs. 4(a) and 4(b), respectively. Since the time-averaged potential increases linearly with the duty cycle, we expect the contrast to increase according to the Boltzmann factor [Eq. (2)]. This is indeed the case, as seen in Fig. 4(a). If we fit the contrast vs duty cycle data using the calculated well depths (as described above for Fig. 3) we obtain a best-fit temperature of 0.7 ± 0.2 mK. For these data, the trap detuning was $-1.3\Gamma_1$, somewhat larger in magnitude than the value ($-1.0\Gamma_1$) used for the detuning data (Fig. 3). This trend of decreasing temperature with increasing detuning is consistent with our MOT temperature measurements [25].

The numerical calculations indicate that, for a fixed detuning, the potential-well depth should increase approximately as the product of the two Rabi rates, i.e., as the square root of the product of the two intensities. Since both beams pass through a single AOM, we control the two intensities by adjusting the rf drive power to the AOM. The data [contrast vs $(I_1I_3)^{1/2}$] are shown in Fig. 4(b). Once again, we include a fit based on the calculated well depths. In this case, the best-fit temperature is 0.8 ± 0.7 mK. The large uncertainty is due to the limited range and precision of the data. The fact that the curve is still increasing at the highest intensities indicates that our measured contrast (i.e., the well depth) is limited by the available laser intensity.

For all of the above data, we operate at a fixed alternation frequency $f\sim 20$ kHz. The measured contrast is independent of f for 5 kHz$<f<$100 kHz. For $f<5$ kHz and $f>100$ kHz the contrast rapidly disappears. At low frequencies, this is due to the diffusion of atoms away from the potential minima when the bichromatic field is off. At high frequencies, the bichromatic field is not on long enough (e.g., <1 μs) to reach steady state (recall that the $5D$ lifetime is ~ 240 ns).

We note that there are conditions (large duty cycle and/or small Δ_1) under which significant contrast is observed but with a reduced number of atoms in the trap. For a fixed duty cycle, the steady-state number of atoms in the trap (determined from time-averaged fluorescence) is symmetric with respect to Δ_1 with a deep minimum at $\Delta_1=0$. If the bichromatic field is turned off, the fluorescence increases with the characteristic loading time of the trap (~ 1 s). The lack of an instantaneous drop in the fluorescence indicates negligible fluorescence (compared to that from the MOT) due directly

to the bichromatic field, in agreement with our OBE calculations. We believe that the reduced number of trapped atoms is not a consequence of the rectified force, but of the manner in which we produce the bichromatic standing wave. In order to compensate for reflection losses, the retroflected beams are slightly smaller than the incoming beams. As a result, outside the central region of the trap, there are intensity imbalances that tend to inhibit the trap loading, especially when the lower transition is near resonance (i.e., $\Delta_1 \sim 0$) and/or the duty cycle is large.

The issues of cooling and heating in this system are important. Calculations for our two-photon resonant cascade situation show [26] that under some conditions sufficient cooling to overcome the heating can be obtained, resulting in stable one-dimensional trapping in the rectified force potential well. However, the strong cooling occurs when the intensities are higher than we have achieved so far in the experiments. If stable trapping (without the need for additional cooling beams) could be realized, bichromatic standing waves could be alternately applied in three dimensions, resulting in a deep three-dimensional trap with cooling, which does not require a magnetic field. Atoms would be confined in a three-dimensional lattice of potential minima which are spaced by the 71-μm beat wavelength. These lattice points are sufficiently separated to be individually optically addressed.

In conclusion, we have observed the rectified dipole force that results when a three-level cascade configuration atom is subjected to a bichromatic standing wave. This force causes cold atoms to accumulate in the resulting macroscopic periodic potential. Experimental results are in reasonable agreement with theoretical expectations. Such rectified forces may prove useful in forming new and deeper laser traps as well as in atom optics applications.

This work was supported in party by NSF (Grant No. PHY-8857336), the University of Connecticut Research Foundation, and the Donors of the Petroleum Research Fund, administered by the American Chemical Society. V.S.-V. acknowledges financial support from the INAOE and the CONACYT (Mexico). We are grateful to S. Maleki for valuable contributions at the early stages of this work.

[1] J. Opt. Soc. Am. B **2**(11) (1985), special issue on the mechanical effects of light, edited by P. Meystre and S. Stenholm.

[2] J. Opt. Soc. Am B **6**(11) (1989), special issue on laser cooling and trapping of atoms, edited by S. Chu and C. Weiman.

[3] Laser Phys. **4**(5) (1994), special issue on laser cooling and trapping, edited by V. Bagnato, N. Bigelow, A. Dykhne, J. Weiner, and Y. Yakovlev.

[4] A. P. Kazantsev and I. V. Krasnov, Pis'ma Zh. Eksp. Teor. Fiz. **46**, 264 (1987) [JETP Lett. **46**, 332 (1987)].

[5] A. P. Kazantsev and I. V. Krasnov, J. Opt. Soc. Am. B **6**, 2140 (1989).

[6] J. Javanainen, Phys. Rev. Lett. **64**, 519 (1990).

[7] A. I. Sidorov, R. Grimm, and V. S. Letokhov, J. Phys. B **24**, 3733 (1991).

[8] M. G. Prentiss, N. P. Bigelow, M. S. Shahriar, and P. R. Hemmer, Opt. Lett. **16**, 1695 (1991).

[9] P. R. Hemmer, M. G. Prentiss, M. S. Shahriar, and N. P. Bigelow, Opt. Commun. **89**, 335 (1992).

[10] R. Grimm, Y. B. Ovchinnikov, A. I. Sidorov, and V. S. Letokhov, Opt. Commun. **84**, 18 (1991).

[11] T. T. Grove and P. L. Gould, Laser Phys. **4**, 957 (1994).

[12] R. Grimm, Y. B. Ovchinnikov, A. I. Sidorov, and V. S. Letokhov, Phys. Rev. Lett. **65**, 1415 (1990).

[13] Y. B. Ovchinnikov, R. Grimm, A. I. Sidorov, and V. S. Letokhov, Opt. Commun. **102**, 155 (1993).

[14] P. R. Hemmer, M. S. Shahriar, M. G. Prentiss, D. P. Katz, K. Berggren, J. Mervis, and N. P. Bigelow, Phys. Rev. Lett. **68**, 3148 (1992).

[15] R. Gupta, C. Xie, S. Padua, H. Batelaan, and H. Metcalf, Phys. Rev. Lett. **71**, 3087 (1993).

[16] R. Grimm, V. S. Letokhov, Y. B. Ovchinnikov, and A. I. Sidorov, Pis'ma Zh. Eksp. Teor. Fiz. **54**, 611 (1991) [JETP Lett. **54**, 615 (1991)].

[17] J. Soding, R. Grimm, J. Kowalski, Y. B. Ovchinnikov, and A. I. Sidorov, Europhys. Lett. **20**, 101 (1992).

[18] E. L. Raab, M. Prentiss, A. Cable, S. Chu, and D. E. Pritchard, Phys. Rev. Lett. **59**, 2631 (1987).

[19] C. Monroe, W. Swann, H. Robinson, and C. Wieman, Phys. Rev. Lett. **65**, 1571 (1990).

[20] K. C. Harvey and C. J. Myatt, Opt. Lett. **16**, 910 (1991).

[21] T. P. Dinneen, C. D. Wallace, and P. L. Gould, Opt. Commun. **92**, 277 (1992).

[22] T. T. Grove, V. Sanchez-Villicana, B. C. Duncan, S. Maleki, and P. L. Gould, Phys. Scr. (to be published).

[23] Assuming a three-level system and parameters typical for the experiment, $\Delta_1 = -\Delta_3 = 1.5\Gamma_1$, $\Omega_1 = 3.1\Gamma_1$, $\Omega_3 = 1.5\Gamma_1$, we calculate that the total fluorescence (at both 780 and 776 nm) during the rectification phase will exhibit a peak-to-peak modulation of 13%. Accounting for the duty cycle (10%), the 780-nm filter transmission, and the fluorescence rate during the MOT phase, we find that this fluorescence modulation could account for a contrast of at most 0.7%, a factor of 10 less than we typically observe.

[24] We use circularly polarized standing waves in an attempt to produce an effective three-state system. However, we find that the measured contrast is relatively independent of this polarization, indicating that the optical pumping during the rectification phase is insufficient to completely transfer atoms to the state of highest m_F. This is not surprising in light of the inhomogeneous magnetic field of the MOT and the fact that the optical pumping must proceed via cascades from the relatively long-lived ($\sim$240-ns) $5D$ level. Therefore, we calculate the Rabi rates assuming the atoms are equally distributed among the hyperfine sublevels.

[25] C. D. Wallace, T. P. Dinneen, K. Y. N. Tan, A. Kumarakrishnan, P. L. Gould, and J. Javanainen, J. Opt. Soc. Am. B **11**, 703 (1994).

[26] H. Pu, T. Cai, N. P. Bigelow, T. T. Grove, and P. L. Gould, Opt. Commun. (to be published).